

# Rational approximations of viscous losses in vocal tract acoustic modeling<sup>a)</sup>

Reiner Wilhelms-Tricarico<sup>b)</sup> and Richard S. McGowan<sup>c)</sup>  
*CReSS LLC, Lexington, Massachusetts 01007*

(Received 17 July 2003; revised 12 March 2004; accepted 22 March 2004)

The modeling of viscous losses in acoustic wave transmission through tubes by a boundary layer approximation is valid if the thickness of the boundary layer is small compared to the hydraulic radius. A method was found to describe the viscous losses that extends the frequency range of the model to very low frequencies and very thin tubes. For higher frequencies, this method includes asymptotically the spectral effects of the boundary layer approximation. The method provides a simplification for the rational approximation of the spectral effects of viscous losses. © 2004 Acoustical Society of America. [DOI: 10.1121/1.1738686]

PACS numbers: 43.72.Ja, 43.75.Ef, 43.75.Np [LLT]

Pages: 3195–3201

## I. INTRODUCTION

Our immediate goal is to realize relatively accurate approximations of viscous effects in digital filter designs that can be used to simulate one-dimensional wave propagation in tubes, such as the vocal tract or certain musical instruments. This paper deals with the following prerequisite for digital simulation: Viscous losses depend on transcendental functions of frequency that must be approximated using rational functions, i.e., ratios of polynomials.

## II. VISCOUS LOSS

### A. Boundary layer approximation

Following Lighthill (Ref. 1, pp. 128–136), we consider fluid flow in a region  $z > 0$  above a wall at  $z = 0$ , with a small spatially uniform pressure gradient  $p_x = \partial p_e / \partial x$  only in the  $x$  direction that oscillates at a circular frequency  $\omega$ . The resulting equilibrium of forces is

$$\rho \frac{\partial u}{\partial t} = -p_x + \mu \frac{\partial^2 u}{\partial z^2} \quad \text{or} \quad -i\omega\rho u + \mu \frac{\partial^2 u}{\partial z^2} = p_x. \quad (1)$$

In the frequency representation, the flow  $u$  varies as  $\exp(i\omega t)$ . A solution to this equation, satisfying the boundary condition  $u(z, \omega) = 0$  for  $z = 0$  and at the same time the condition of being finite for  $z \rightarrow \infty$ , is the following:

$$u(z, \omega) = -\frac{p_x}{i\omega\rho} \left[ 1 - \exp\left(-\sqrt{\frac{i\omega\rho}{\mu}} z\right) \right]. \quad (2)$$

For  $z \rightarrow \infty$  the particle velocity,  $u(z, \omega)$ , reduces to the flow without rotation that would have been obtained if the viscosity was neglected:  $u_0 = -p_x / (i\omega\rho)$ . This equation is approximately correct for axial acoustic flow in a duct with sufficiently large cross-sectional area  $A_0$ . That is, for a given frequency  $\omega$  the value of  $z$  at which the exponential in the equation becomes nearly zero should be small compared to

the hydraulic radius  $R = \sqrt{A_0/\pi}$ . This is the boundary layer approximation. To obtain the rate of the volume flow  $U$  in tube of cross-sectional area  $A_0$ , the flow field needs to be integrated over the tract's cross-sectional area:

$$U(\omega) = -\frac{p_x}{i\omega\rho} \left[ A_0 - \int_{A_0} \frac{p_x}{i\omega\rho} \exp\left(-\sqrt{\frac{i\omega\rho}{\mu}} z\right) dA \right]. \quad (3)$$

If the boundary layer is thin compared to the hydraulic radius, the integration of the exponential can be carried out from the boundary wall to infinity, and multiplied by the circumference of the tract. The result is

$$U(s) = -p_x(s) \frac{A_0}{\rho} \frac{1}{s} \left[ 1 - \frac{S_0}{A_0} \sqrt{\frac{\nu}{s}} \right], \quad (4)$$

where now  $s$  replaces  $i\omega$  as the generalized frequency variable, so that  $U(s)$  represents the Laplace transform of the volume velocity, and  $\nu = \mu/\rho = 0.168 \text{ cm}^2/\text{s}$  is the kinematic viscosity in air at 37 °C. This boundary layer approximation breaks down at low frequencies and/or small cross-sectional areas. For these situations the imposed pressure gradient is largely balanced by viscous stress over most of the cross-sectional area. Two distinct duct shapes are considered in the following: the rectangular duct and cylindrical duct.

### B. Symmetric flow in a flat rectangular duct

In a shallow duct that has an area  $A_0 = 2Rb$ , with  $b \gg R$ , and where  $R$  is half the height and  $b$  is the cross length of the duct, it is reasonable to assume that the flow is maximal near the geometrical center of the duct, as shown in Fig. 1.

Let  $z$  be a variable that parametrizes the rectangular duct cross section as follows:  $z$  is zero at the center plane and becomes equal to  $R$  at one of the walls. Assuming that the flow is symmetric, the following constraints hold:  $u(R) = 0$  as before, and  $u'(0) = 0$ , and the unique solution to Eq. (1) is

$$u(r, s) = -\frac{1}{s\rho} p_x \left( 1 - \frac{\cosh(z\sqrt{s/\nu})}{\cosh(R\sqrt{s/\nu})} \right), \quad (5)$$

<sup>a)</sup>A preliminary version was presented at the 145th Meeting of the Acoustical Society of America as poster 5aSC22, titled "Padé approximations for boundary-layer losses in articulatory synthesis."

<sup>b)</sup>Electronic mail: rew@cressl.com

<sup>c)</sup>Electronic mail: rsmcgowan@cressl.com

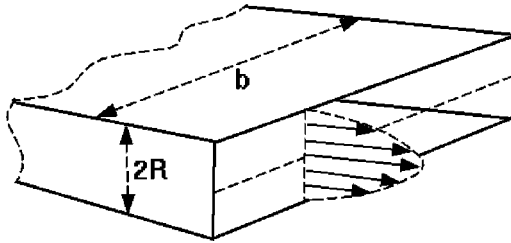


FIG. 1. Expected symmetrical flow through a narrow rectangular duct.

again replacing  $i\omega$  by  $s$ . For sufficiently high frequencies or large cross sections of the duct, the cosh-flow profile looks very much like that of the boundary layer approximation, Eq. (2), but for low frequencies or small  $R$  they differ considerably (Fig. 2).

### C. Flow in a cylindrical duct

The other extreme case is that of a small cylindrical cross section. Written in cylindrical coordinates with the assumption of circular symmetry the momentum conservation equation, Eq. (1) from above, becomes

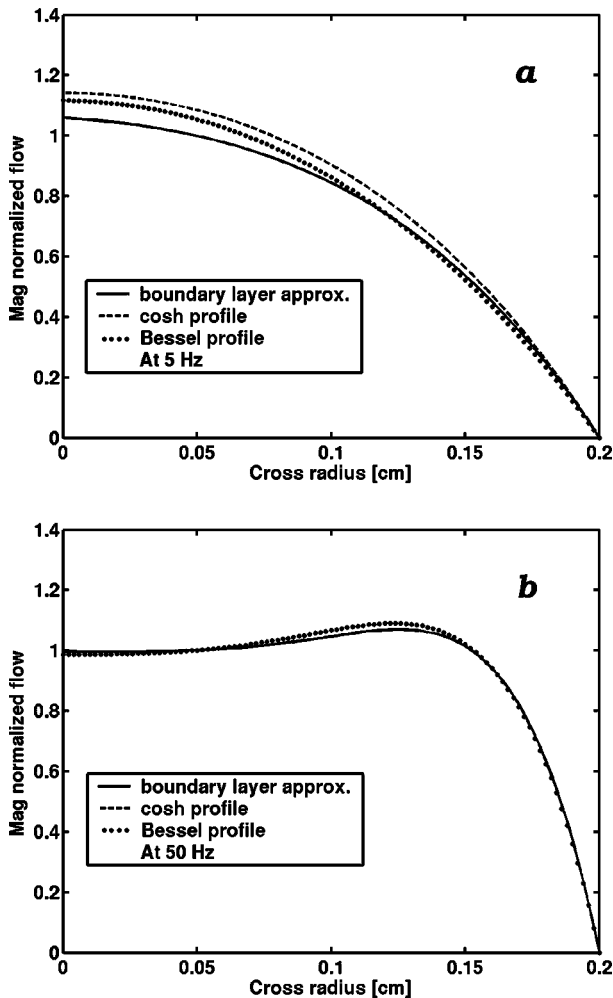


FIG. 2. The three flow profiles for the in-the-boundary layer for 5 Hz (a) and 50 Hz (b). The wall is to the right in each case, where the flow is zero. In the computation, the term  $-p_x/(\rho s)$  in  $u(r,s)$  was dropped for normalization.

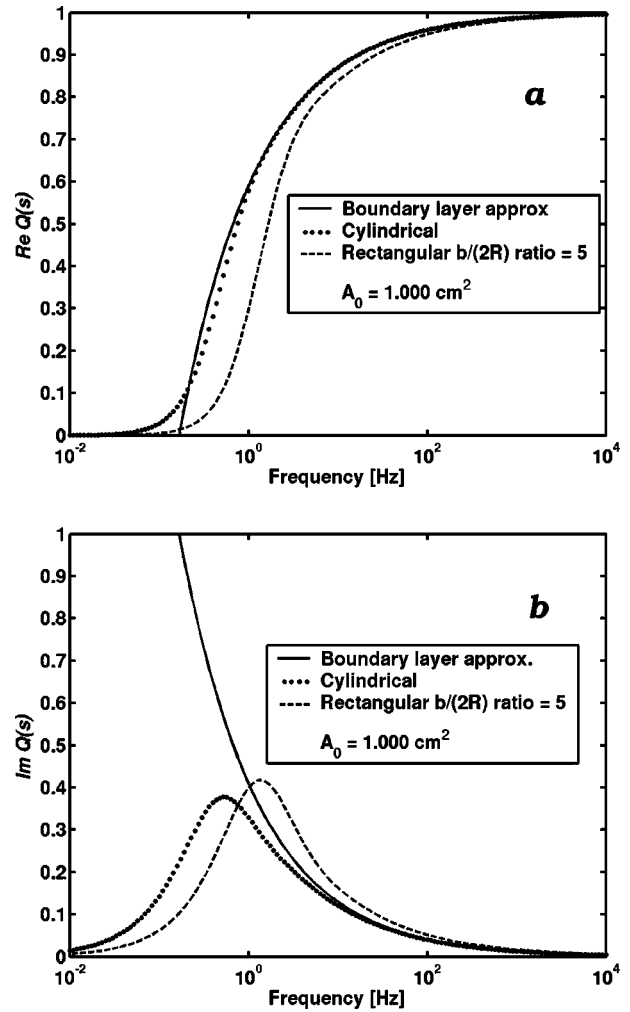


FIG. 3. Real (a) and imaginary part (b) of the damping factor function  $Q(s)$ .

$$-s\rho u + \mu \left( \frac{\partial^2 u}{\partial r^2} + \frac{1}{r} \frac{\partial u}{\partial r} \right) = p_x. \quad (6)$$

In this case,  $r$  is a parameter that is zero at the center of the duct and becomes  $R$  at the walls. Changing the variable to  $z = r\sqrt{s/\nu}$ , this equation can be transformed into a modified Bessel equation of zeroth order (see Ref. 2, p. 374, 9.6.1). Using only solutions that have no singularity at zero, and taking the nonslip condition  $u(R) = 0$  into account, the solution becomes

$$u(r,s) = -\frac{1}{s\rho} p_x \left( 1 - \frac{I_0(r\sqrt{s/\nu})}{I_0(R\sqrt{s/\nu})} \right). \quad (7)$$

Here  $I_0(x)$  represents the modified (or hyperbolic) Bessel function of the first kind of zeroth order. Again, for sufficiently high frequencies, or large cross sections, this solution looks like the other two, as is seen in Fig. 2.

### D. Volume velocities

Volume velocities are obtained by integrating the axial particle velocity over the cross-sectional area of the duct. In the case of the rectangular channel (see Fig. 1), ignoring the effects at the wall of the small sides, the result is

$$U_R(s) = -p_x(s) \frac{A_0}{s\rho} \left( 1 - \frac{\tanh(R\sqrt{s/\nu})}{R\sqrt{s/\nu}} \right), \quad (8)$$

where the change of variables  $R=A_0/(2b)$  was used to eliminate  $b$ .

For the case of a cylindrical duct, the flow given by Eq. (7) is integrated over a disk, with  $RS_0/A_0=2$ . This and the fact that  $\int_0^y I_0(x) dx = yI_1(y)$ , where  $I_1(y)$  represents the first-order modified Bessel function of the first kind, can be used to obtain

$$U_C(s) = -p_x(s) \frac{A_0}{s\rho} \left( 1 - 2 \frac{I_1(R\sqrt{s/\nu})}{R\sqrt{(s/\nu)I_0(R\sqrt{s/\nu})}} \right). \quad (9)$$

All three expressions for volume velocity (4), (8), and (9) are of the form  $U(s) = -p_x(s)(A_0/s\rho)Q(s)$  where  $Q(s)$  is a frequency-dependent damping factor. The following three versions of  $Q(s)$  are shown in Fig. 3:

$$Q(s) = \begin{cases} 1 - \frac{2}{R\sqrt{s/\nu}} & (10a) \\ 1 - \frac{\tanh(R\sqrt{s/\nu})}{R\sqrt{s/\nu}} & (10b) \\ 1 - 2 \frac{I_1(R\sqrt{s/\nu})}{R\sqrt{(s/\nu)I_0(R\sqrt{s/\nu})}} & (10c) \end{cases}$$

[Eq. (10a) boundary layer approximation, Eq. (10b) rectangular duct, Eq. (10c) cylindrical duct]. As can also be seen in Fig. 3, the third form of  $Q(s)$  [Eq. (10c), dotted graph] including the Bessel functions approaches the first form [Eq. (10a), solid graph] and according to Eq. (4), already for relatively low frequencies (the frequency scales are logarithmic to emphasize the difference between the curves for low frequencies). For the rectangular case [Eq. (10b), dashed graph in Fig. 3] the ratio of 5 between sides was used. The curves

are located more to the right for higher values of the ratio and to the left for lower value, while the maximal similarity (but not identity) between cases (b) and (c) can be found for a ratio of about 2.

### III. EFFECTS ON VOCAL TRACT TRANSFER FUNCTION

For a tube with a time-constant cross-sectional area  $A(x)$ , the Laplace transform,  $p(x,s)$ , of the pressure, and  $U(x,s)$  of the volume velocity obey the following differential equations (see also Ref. 3):

$$\begin{aligned} \frac{d}{dx} p(x,s) &= -s \frac{\rho}{A(x)} U(x,s), \\ \frac{d}{dx} U(x,s) &= -s \frac{A(x)}{\rho c^2} p(x,s). \end{aligned} \quad (11)$$

This system can be written in matrix form while including  $Q(s)$ , which now is written as  $Q(x,s)$  in order to represent its dependence upon the cross-sectional area at  $x$  via the hydraulic radius  $R$  [see Eq. (10)]:

$$\begin{aligned} \frac{d}{dx} \begin{pmatrix} p(x,s) \\ U(x,s) \end{pmatrix} &= L(x,s) \begin{pmatrix} p(x,s) \\ U(x,s) \end{pmatrix} \\ &= \begin{pmatrix} 0 & -s \frac{\rho}{A(x)} \frac{1}{Q(x,s)} \\ -s \frac{A(x)}{\rho c^2} & 0 \end{pmatrix} \\ &\quad \times \begin{pmatrix} p(x,s) \\ U(x,s) \end{pmatrix}. \end{aligned} \quad (12)$$

By calculating the matrix exponent of  $\Delta x L(x,s)$ , shown above, a propagation matrix for a constant area tube segment of length  $\Delta x$  is obtained. It transforms variables at one end of a segment with constant properties of length  $\Delta x$  to the variables on the other end,

$$\begin{pmatrix} p(x+\Delta x,s) \\ U(x+\Delta x,s) \end{pmatrix} = \begin{pmatrix} \cosh(\phi(x,s)) & -\frac{1}{Y(x,s)} \sinh(\phi(x,s)) \\ -Y(x,s) \sinh(\phi(x,s)) & \cosh(\phi(x,s)) \end{pmatrix} \begin{pmatrix} p(x,s) \\ U(x,s) \end{pmatrix}, \quad (13)$$

using the following functions, evaluated at point  $x$ :

$$\text{propagation phase: } s \frac{\Delta x}{c} \rightarrow \phi(x,s) = \frac{\Delta x}{c} \frac{s}{\sqrt{Q(x,s)}}, \quad (14)$$

$$\text{admittance: } \frac{A(x)}{\rho c} \rightarrow Y(x,s) = \frac{A(x)}{\rho c} \sqrt{Q(x,s)}. \quad (15)$$

The transfer function of, for example, a vocal tract can then be obtained by multiplying the partial chain matrices, while accounting for the radiation impedance. To be able to compare the effects of viscous losses for different geometries, we make the assumption that a piece of tube is terminated with a simplified radiation impedance, which is obtained as a low order frequency approximation of radiation load of a piston set in an infinite plane baffle (see, for example, Ref. 3). The radiation impedance is

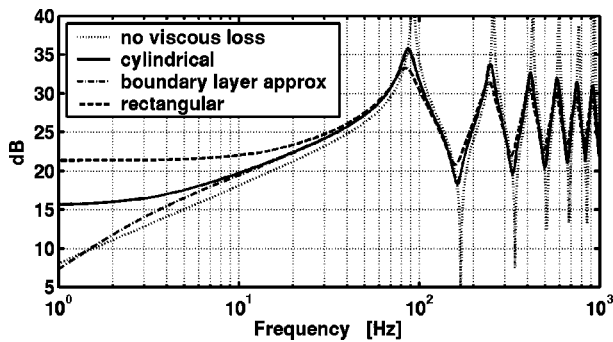


FIG. 4. Input impedance of a thin exponential tube of 100 cm length, modeled by 25 constant segments of equal length. The area starts from 0.1 cm<sup>2</sup> and ends at 0.1492 cm<sup>2</sup>. The radiation impedance is calculated from the final segment's area. The curve with the highest peaks (dots) is input impedance with no viscous loss, the other curves are obtained by taking the viscous loss into account using three different models. The curve for the rectangular cross sections is calculated for a length ratio of 1:8.

$$Z_{\text{rad}}(s) = \frac{\rho c}{\pi a^2} \frac{(8a/3\pi c)s}{1 + (3\pi a/16c)s}$$

where  $a$  is the piston radius. (16)

As commonly done, we denote the elements of the duct's propagation matrix as  $\begin{pmatrix} A & B \\ C & D \end{pmatrix}$ , which can be obtained by multiplying the individual propagation matrices of all segments together. Its determinant is equal to 1 since it is obtained as product of matrices of the type shown in Eq. (13). The volume velocity transfer function,  $H(s)$ , defined here as the ratio of volume flow at the radiating end of the tube divided by volume flow across the beginning, and the input impedance  $Z_{\text{in}}(s)$ , are

$$H(s) = \frac{1}{A - CZ_{\text{rad}}} \quad \text{and} \quad Z_{\text{in}}(s) = \frac{DZ_{\text{rad}} - B}{A - CZ_{\text{rad}}}. \quad (17)$$

Figure 4 shows the input impedance for a very thin exponential horn that has either circular cross sections or rectangular cross sections. In both cases, the cross-sectional areas vary from 0.1 to 0.1492 cm<sup>2</sup> exponentially; in the cylindrical case the hydraulic radius  $R$  varies from 0.1784 to 0.2179 cm, and  $R$  varies from 0.0559 to 0.0683 cm in the rectangular case (where the ratio of long to short side was set to 8). For such small cross sections and hydraulic radii we expect a strong effect of the viscous losses and differences among the three different situations. In order to separate the effects of viscous losses from the effects of losses by radiation, the same radiation impedance, namely that of a circular piston, is used in

all cases. It can be seen that the two curves for the cylindrical tube, one resulting from the boundary layer approximation, using the square-root of  $s$  in  $Q(s)$ , and the other using modified Bessel functions, are very nearly the same for frequencies as low as 50 Hz.

#### IV. RATIONAL APPROXIMATION AND DIGITAL FILTERS

The three expressions for  $Q(s)$  can be used to obtain an analytical description of the volume velocity over frequency, while a digital filter implementation to simulate vocal tract acoustics requires rational expressions. The three representations of  $Q(s)$  that have been considered here involve a square root of frequency law for the boundary layer approximation, hyperbolic functions, or hyperbolic Bessel functions. These result in nearly the same influence on the transfer function. However, the rational approximations of the latter two functions are more easily obtained than for the square root-of-frequency dependence. This is because  $\sqrt{x}$  possesses an essential singularity at zero, while the two other functions have only isolated singularities.

For the case of the function  $[\tanh(x)]/\sqrt{x}$ , a straightforward method of implementation as a filter can be based on the infinite product representation of the  $\sinh x$  and  $\cosh x$ : The function  $\sinh x$  has zeros at 0 and at  $\pm ik\pi$ ,  $k=1, \dots, \infty$ , and  $\cosh x$  has zeros at  $\pm i(2k-1)\pi$ ,  $k=1, \dots, \infty$ . Since the zero of  $\sinh x$  at zero is eliminated by  $1/x$ ,

$$\begin{aligned} \frac{\tanh x}{x} &= \frac{\sinh x}{x \cosh x} \\ &= \prod_{k=1}^{\infty} \frac{1 + x^2/k^2\pi^2}{1 + 4x^2/(2k-1)^2\pi^2}, \quad \text{therefore:} \\ \frac{\tanh \sqrt{x}}{\sqrt{x}} &= \prod_{k=1}^{\infty} \frac{1 + x/k^2\pi^2}{1 + 4x/(2k-1)^2\pi^2}. \end{aligned} \quad (18)$$

A digital filter can then be obtained by truncating the product at some finite  $N$  and replacing the Laplace variable  $s$  by a bilinear transform,

$$s \rightarrow 2f_s \frac{1 - z^{-1}}{1 + z^{-1}} \quad \text{whereby } f_s \text{ is the sampling frequency.} \quad (19)$$

The resulting approximation of  $Q(s)$  of Eq. (10b) is a series of stable bilinear filters with poles at

$$\frac{4\alpha - (2k-1)^2\pi^2}{4\alpha + (2k-1)^2\pi^2} \quad \text{with } \alpha = \frac{R^2}{\nu} \cdot 2f_s:$$

$$Q(s) \rightarrow 1 - \prod_{k=1}^N \left( \frac{2k-1}{k} \right)^2 \frac{(\alpha + k^2\pi^2) - (\alpha - k^2\pi^2)z^{-1}}{(4\alpha + (2k-1)^2\pi^2) - (4\alpha - (2k-1)^2\pi^2)z^{-1}}. \quad (20)$$

It should be noted that all poles of the resulting digital filter lie within the unit circle. Figure 5 shows a comparison of magnitude of the exact function  $Q(s)$  for a case of a rectan-

gular duct with two approximations by five and ten product terms.

The convergence of the product type of approximation is

somewhat slow. Better methods are based on Padé approximations or continued fraction expansions (see Ref. 4). In short, the  $[L/M]$  Padé approximation of a function  $f(s)$  is a rational function with numerator degree  $L$  and denominator degree  $M$  which best represents a  $M+L+1$ -degree series approximation (e.g., Taylor or MacLaurin) of the function. (Working implementations of this method can be found in Maple or in the Mathematica software which was used in this work.) The rational approximation of the function  $Q(s)$  by Padé approximants has strong advantages over Taylor or MacLaurin series approximation because of a considerably wider range of close approximation. The representation in digital filters is obtained in two steps: (a) approximation of the transcendental functions by rational function in the generalized frequency, or  $s$ , domain; (b) mapping of the resulting rational functions into digital filters by means of the bilinear transform.

Rational approximants for the functions  $Q(s)$  are then found based on, for example, a  $[4/6]$  Padé approximation:

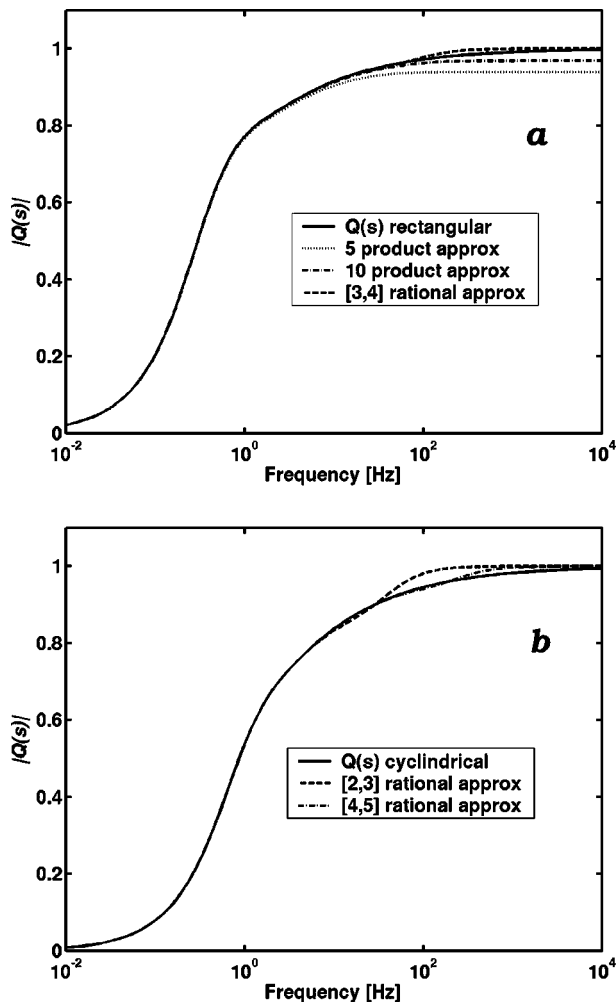


FIG. 5. Magnitudes of the function  $Q(s)$  and its approximations. (a) The case of a rectangular cross section. The  $[3, 4]$  rational approximation (uppermost dashed curve) is based on the  $[6/8]$  Padé approximation of  $\tanh(x)/x$ . (b) Circular cross section. The  $[2, 3]$  and  $[4, 5]$  rational approximations result from  $[4/6]$  and  $[8/10]$  Padé approximations of  $I_1(x)/xI_0(x)$ .

$$\frac{\tanh(R\sqrt{s/\nu})}{R\sqrt{s/\nu}} \approx \frac{1 + \frac{4}{33}x + \frac{1}{495}x^2}{1 + \frac{5}{11}x + \frac{2}{99}x^2 + \frac{1}{10395}x^3}$$

with  $x = \frac{R^2}{\nu} s$ . (21)

Similarly,

$$\frac{I_1(R\sqrt{s/\nu})}{R\sqrt{s/\nu} I_0(R\sqrt{s/\nu})} \approx \frac{1}{2} \frac{1 + \frac{1}{12}x + \frac{1}{960}x^2}{1 + \frac{5}{24}x + \frac{1}{160}x^2 + \frac{1}{46080}x^3}$$

with  $x = \frac{R^2}{\nu} s$ . (22)

Note that both functions being approximated are even functions, and, thus, only even powers of their arguments appear in the Padé approximation.

It is also possible to use the continued fraction expansion (CFE) of the above expressions (Ref. 4, pp. 175–177). The following CFEs, if truncated as shown, are equivalent to the  $[4/6]$  Padé approximants:

$$\frac{\tanh\sqrt{x}}{\sqrt{x}} = \frac{1}{1 + \frac{x}{3 + \frac{x}{5 + \frac{x}{7 + \frac{x}{9 + \frac{x}{11 + \dots}}}}}} \quad (23)$$

and

$$\frac{I_1(\sqrt{x})}{\sqrt{x}I_0(\sqrt{x})} = \frac{1}{2 + \frac{x}{4 + \frac{x}{6 + \frac{x}{8 + \frac{x}{10 + \frac{x}{12 + \dots}}}}} \quad (24)$$

The CFE for  $\tanh$ , from which Eq. (23) is obtained, can be found in Ref. 2 (p. 75, 4.3.94). To obtain Eq. (24), the continued fraction expansion of  $J_1(x)/J_0(x)$  given in Ref. 4 was transformed to obtain the above CFE for the expression with the modified Bessel functions. Since these CFEs are valid also for  $x=0$ , the essential singularity at 0 caused by the square root in the boundary layer approximation is not present in these approximations.

A simple transformation of the expressions (23) and (24), obtained by dividing every other fraction of the CFE by  $x$ , yields an electrical network whose input impedance is equal to the approximated functions above. This electrical network structure is shown in Fig. 6.

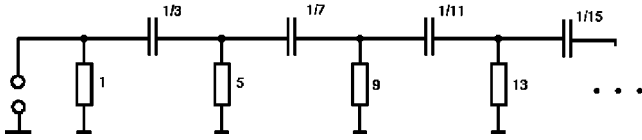


FIG. 6. The input impedance of the electrical network shown here approximates  $\tanh \sqrt{s}/\sqrt{s}$  [see Eq. (23)], since the CFE of this function can be rewritten as

$$1 + \frac{1}{3/s + \frac{1}{5 + \frac{1}{7/s + \frac{1}{9 + \frac{1}{11/s + \frac{1}{13 + \dots}}}}}}$$

## V. SKETCH OF A DIGITAL IMPLEMENTATION

The implementation of a digital simulation of wave guide acoustics in the time domain is accomplished by for-

$$G(x,s) = \begin{pmatrix} \cosh\left(\frac{\Delta x}{c} \frac{s}{\sqrt{Q}}\right) - \frac{1+Q}{2\sqrt{Q}} \sinh\left(\frac{\Delta x}{c} \frac{s}{\sqrt{Q}}\right) & -\frac{Q-1}{2\sqrt{Q}} \sinh\left(\frac{\Delta x}{c} \frac{s}{\sqrt{Q}}\right) \\ \frac{Q-1}{2\sqrt{Q}} \sinh\left(\frac{\Delta x}{c} \frac{s}{\sqrt{Q}}\right) & \cosh\left(\frac{\Delta x}{c} \frac{s}{\sqrt{Q}}\right) + \frac{1+Q}{2\sqrt{Q}} \sinh\left(\frac{\Delta x}{c} \frac{s}{\sqrt{Q}}\right) \end{pmatrix} \quad (26)$$

Since  $\sinh$  is an odd function and  $\cosh$  is an even function of its argument, the square root,  $\sqrt{Q(s,x)}$ , never appears or can be canceled in rational approximations of the above expressions. For example, using the [5/5] Padé of  $\sinh$ , the following rational approximation is obtained:

$$\frac{1+Q}{2\sqrt{Q}} \sinh\left(\frac{\Delta x}{c} \frac{s}{\sqrt{Q}}\right) \approx \frac{1+Q}{2} \frac{s \left( \Delta x/c + \frac{53}{396} (\Delta x/c)^3 s^2/Q + \frac{551}{166320} (\Delta x/c)^5 s^4/Q^2 \right)}{1 - \frac{13}{396} (\Delta x/c)^2 s^2/Q + \frac{5}{11088} (\Delta x/c)^4 s^4/Q^2}. \quad (27)$$

Similar expressions containing rational functions with powers of  $s$  and  $Q(x,s)$  are obtained for the other components of  $G(x,s)$ .

The transformation into digital filters then requires the implementation of a rational approximation and bilinear transformation of the filter  $s/Q(s,x)$ , and powers of this filter are obtained by cascading the same filter structure. The analog filter with transfer function  $s/Q(s,x)$  is a differentiator (multiplication by  $s$ ) followed by one of the two CFEs [Eqs. (23) or (24)] in a feedback loop.

The absolute value of the input impedance of the two passive electrical networks (see Fig. 6) is limited from above by 1. Therefore, an analog system with these networks in the feedback loop must be stable. In fact, it can be shown by induction that for all truncated CFEs of this form, all except one pole of the approximated filter  $s/Q(s,x)$  are on the negative real axis and one pole is at  $s=0$ . The bilinear transform (19) renders directly the rational functions in the approximation of  $G(x,s)$  into digital filters. Note that the coefficients

wards and backwards traveling waves, sampled at a sampling time interval that is proportional to tube segment length. While in the lossless Kelly–Lochbaum model (Ref. 5) the traveling waves in each segment are represented by simple delay elements, for frequency-dependent viscous loss these are replaced by more general digital filters.

The transformation from pressure and volume flow representation to forward and backward traveling waves is given by

$$\begin{pmatrix} V^+ \\ V^- \end{pmatrix} = R(x) \begin{pmatrix} p \\ U \end{pmatrix} = \begin{pmatrix} 1 & \frac{c\rho}{A(x)} \\ 1 & -\frac{c\rho}{A(x)} \end{pmatrix} \begin{pmatrix} p \\ U \end{pmatrix}. \quad (25)$$

Using the above transformation from left and right, the ABCD matrix of a segment is transformed into a transmission matrix that relates forward and backward traveling waves at the beginning and end of a segment of length  $\Delta x$  [for brevity  $Q(x,s)$  is written as  $Q$ ]:

$\Delta x/c$  are cancelled if the sampling frequency is chosen as  $f_s = c/\Delta x$ .

The structure of a digital filter corresponding to the analog filter  $s/Q(s,x)$  is a lattice structure that can be derived by replacing the variable  $s$  by the bilinear transform and by using Euler's recursion (see Ref. 4, p. 125) for the evaluation of continued fractions. The bilinear transformation preserves the stability property. The resulting structure has one delay-free path which can be eliminated by generalizing a method that was shown for a special class of filters in Ref. 6. The practical implementation and verification of these digital filters is currently a work in progress.

## ACKNOWLEDGMENT

This work was supported by Grant No. NIDCD-01247 to CReSS LLC.

- <sup>1</sup>J. Lighthill, *Waves in Fluids* (Cambridge U. P., Cambridge, 1978).
- <sup>2</sup>M. Abramowitz and I. A. Stegun (eds.), *Handbook of Mathematical Functions* (Dover, New York, 1965), SCI QA3.U58 No. 55, 1965.
- <sup>3</sup>M. R. Portnoff, "A Quasi-One-Dimensional Digital Simulation for the Time-Varying Vocal Tract," Master thesis, MIT, 1973.
- <sup>4</sup>G. A. Baker, Jr. and P. Graves-Morris, *Padé Approximants*, 2nd ed. (Cambridge U. P., Cambridge, 1996).
- <sup>5</sup>J. L. Kelly, Jr. and C. Lochbaum, "Speech synthesis," in *Proceedings of the Stockholm Speech Communications Seminar* (RIT, Stockholm, Sweden, 1962).
- <sup>6</sup>A. Härmä, "Implementation of frequency-warped recursive filters," *Signal Process.* **80**, 543–548 (2000).